Enhanced low C/N nitrogen removal in an innovative microbial fuel cell (MFC) with electroconductivity aerated membrane (EAM) as biocathode

Yun Wu[a*, b, c], Qing Yang[b], Qingnan Zeng, Huu Hao Ngo[c*,a], Wenshan Guo[c], Hongwei Zhang[a, b]

[a] *State Key Laboratory of Separation Membranes and Membrane Processes, Tianjin Polytechnic University, Tianjin 300387, China*

[b] *School of Environmental and Chemical Engineering, Tianjin Polytechnic University, Tianjin 300387, China*

[c] *Centre for Technology in Water and Wastewater, School of Civil and Environmental Engineering, University of Technology Sydney, Broadway, NSW 2007, Australia*

*Corresponding authors:

Email: wucloud@163.com; Tel: +86-13820489466

Email: ngohuuhao121@gmail.com; Tel: +61-295142745

.

Abstract

A novel microbial fuel cell (MFC) was developed to enhance simultaneous nitrification and denitrification (SND) by employing electrons from the anode. The cathode chamber of the reactor consisted of a membrane aerated biofilm reactor (MABR) which was made of an electroconductivity aerated membrane. The maximum power density of 4.20 ± 0.12 W m^{-3} was obtained at a current density of 4.10 ± 0.11 A m^{-2} (external resistance = 10 Ω). Compared with an open-circuit system, the removal rates of NH_4^+-N and TN were improved by 9.48 ± 0.33% and 19.80 ± 0.84%,

respectively, which could be ascribed to the electrochemical denitrification. The anode (chemical oxygen demand, COD) and cathode (NO_3^-) chambers reached the maximum coulombic efficiencies (CEs) of 40.67 ± 1.05% and 42.84 ± 1.14%, respectively. It suggested that the electroconductivity MABR has some advantages in controlling aeration intensity, thus improving SND and CEs. Overall, EAM-MFC could successfully generate electricity from wastewater whilst showing high capacity for removing nitrogen at a low COD/N ratio of 2.8 ± 0.07 g COD g^{-1} N.

Keywords: Microbial fuel cell; Biocathode; Membrane aerated biofilm reactor; Simultaneous bio-electrochemical denitrification; Competition of electron acceptors

1. Introduction

Microbial fuel cell (MFC) is a promising novel and environmentally friendly technology for wastewater treatment and energy production [1, 2, 3, 4]. The anaerobic bacteria degrade organic materials and produce electrons, while the electrons migrate to the cathode via an external circuit. The most commonly used electron acceptor is oxygen because it can be combined with protons from the anode to generate water as a non-toxic product. Since Clauwaert [5] first used nitrate as an electron acceptor and successfully achieved complete denitrification, this has attracted increasing attention on nitrogen being removed by MFC biocathode.

Virdis [6] added an external nitrification reactor between the anode and cathode of MFC and the effluent enters into the aerobiotic cathode chamber to accomplish complete nitrogen removal. The removal rate of COD and nitrate was 2 kg COD m^{-3}

NCC d^{-1} and 0.41 kg NO_3^--N m^{-3} NCC d^{-1}, respectively. The electrons provided by the anode can obviously reduce the additional carbon dosing being required for completing denitrification, subsequently achieving a lower COD/N to 4.5 g COD g^{-1} N. However, the reactor design was complex and its construction was expensive. In their further study, they supplied synthetic wastewater to the anode while the effluent was subsequently directed to the cathode. When the COD/N was 3.02 g g^{-1}, the removal rate was achieved the maximum of 77.7%. Thereafter, Yu [7] designed a membrane-aerated MFC compared with a diffuser-aerated MFC, showing that membrane-aerated MFC was better at removing pollutants such as COD and nitrogen. However, the maximum voltage output was just 0.25 V with the calculated coulombic efficiencies between 0.07 and 0.21% which was mainly caused by the oxygen diffuse to anode chamber. The power density produced by recent coupled system was 2, 20 and 465 mW m^{-2} [8, 9, 10]. In the study by Wang [11], a coupled system of MBR and MFC was applied to generate power and remove nutrient. They found the maximum power density reached 6.0 W m^{-3}. Their results indicated that the removal rate of NH_4^+-N could reach over 90%, but the use of stainless steel mesh as the cathode increased excess oxygen, resulting in a low removal rate of TN.

This was similar to Munch [12] who reported efficient simultaneous nitrification and denitrification (SND) at low dissolved oxygen levels (< 0.5 mg L^{-1}), while Pochana and Keller [13] observed complete SND at dissolved oxygen levels ranging between 0.3 and 0.8 mg L^{-1}. In addition, Wang [11] reported a novel coupled system of MFC and MBR, in which low-cost materials guaranteed the effluent's quality. However, sometimes it caused other problems; for example the increase in dissolved oxygen levels in the anode chamber as a result of dissolved oxygen diffusing from the cathode

chamber to the anode chamber led to a low coulombic efficiency (CE) (only 1.5%). This outcome was also reported by Logan [2]. Moreover, Zhu [14] investigated a double-chamber microbial fuel cell (MFC) with a decomposed cyanobacteria solution as the feed to achieve SND. The removal efficiencies of TN and NH_4^+-N were 0.064 ± 0.005 kg m^{-3} day^{-1} and 0.063 ± 0.005 kg m^{-3} day^{-1}, respectively under a closed-circuit scenario (2.6 and 2.0 times compared to those under the open-circuit state, respectively). This indicated the enhanced nitrogen removal rate in the MFC. Yet the removal rate was quite small. To sum up, dissolved oxygen is the common factor for both SND [15, 16] and coulombic efficiency of MFC.

Membrane aerated biofilm reactor (MABR) has some outstanding advantages compared with the above-mentioned systems for the control of dissolved oxygen and nitrogen removal. A counter-diffusion system could be provided by the MABR in which oxygen transferred from the bottom of the biofilm, while organic carbon reverse transmits from the bulk liquid into the biofilm [7]. It was enabled the proper environment for SND processes [17]. However, the amount of nitrogen removed was still limited by the supply of carbon source to denitrification. Furthermore, there are some results that confirmed bioelectrochemical denitrification could further improve nitrogen removal in carbon felt MFC [18, 19]. In addition, the other membrane bioreactor coupled with MFC also led to membrane fouling mitigation [20, 21]. In this study, electroconductivity MABR was coupled with MFC to form the cathode chamber, which realized flexible control of oxygen for efficient SND and higher coulombic efficiency. The electrons that were produced through degrading organic matters by microorganisms at the anode transferred to the cathode where nitrate and nitrite were reduced. Considering that the redox potential of O_2/H_2O (+ 0.82 V) was higher than

NO_3^-/0.5 N_2 (+ 0.74 V) redox potential, oxygen may compete with nitrate to acquire electrons. It led to limited bioelectrochemcial denitrification [22]. As a consequence, electroconductivity MABR will enhance nitrogen removal by bioelectrochemical synergy and control aeration within a proper range when competing for electron acceptors.

In this study, the coupled electroconductivity aerated membrane-microbial fuel cell (EAM-MFC) system was evaluated in terms of electricity generation performance, COD and nitrogen removal and coulombic efficiency. A comparison on COD, NH_4^+-N, NO_3^--N, NO_2^--N removal rates was made between the closed and open circuits to verify whether the nitrogen removal rate could further be improved by electrochemical denitrification in EMA-MFC. The influence of different external loads on nitrogen and carbon removal was assessed. The aeration intensity of electroconductivity MABR was also considered for investigating the advantages of electroconductivity MABR as a cathode to improve SND and coulombic efficiency. Furthermore, the relationship between electrochemical denitrification rate and current density was also examined to analyze the competition among different types of electron acceptors.

2. Methods

2.1. Reactor design and construction

The EAM-MFC coupled system is shown in Fig. 1. This system was constructed with two identical cylinder chambers made of plexiglass (1 L volume each), separated by two cation exchange membranes (CEM, 28.26 cm^2, Ultrax CMI-7000, Membranes International, USA). Before it was used, the anode carbon felt was pretreated by being submerged overnight in 1 M HCl, 1 M NaOH and deionized water, respectively, to

eliminate the effects of other impurities. The cathode chamber utilized an electroconductivity MABR (constructed from electroconductivity aerated membrane) which connected with anode electrodes via an external circuit. The synthetic wastewater was supplied to the cathode chamber using a peristaltic pump (NatongBL-100C, China) at flow rate of 1.39 mL min^{-1} and operated in a continuous mode (HRT = 12 h). electroconductivity MABR used an airflow rotameter to adjust the aeration's intensity. The dissolved oxygen of the cathode liquor was controlled at 0.2-0.5 mg L^{-1} throughout the study, in order to prevent dissolved oxygen diffusing to the anode chamber.

Fig. 1.

2.2. Inoculation and operation of the system

The coupled system was inoculated and fed by synthetic wastewater under intermittent operation mode within first 30 days (the inoculation period), resulting in the formation of an anodic biofilm and a cathodic biofilm. The anodic biofilm was comprised of electricity-producing microbes, while a cathodic biofilm consisted of nitrifying and denitrifying bacteria. The anode and cathode chambers were inoculated with 200 mL of anaerobic sludge and 200 mL of facultative anaerobic sludge, respectively. The facultative anaerobic sludge was obtained as a result of an enrichment transfer procedure over a three-month period at our laboratory via A/O technology. The synthetic wastewater composition (L^{-1}) was: 0.38 g NaAc, 0.3 g NH_4Cl, 0.015 g KH_2PO_4, 11.4 mg $CaCl_2$; 12 mg $MgSO_4$ and 1 mL of trace element solution [23]. The trace solution was consisted of (per litre): 1.5 g $FeC13{\cdot}6H_2O$, 0.15 g H_3BO_3, 0.03 g $Cu_5SO_4{\cdot}5H_2O$, 0.18 g KI, 0.12 g $MnC1_2{\cdot}4H_2O$, 0.06 g $Na_2MoO_4{\cdot}\ 2H_2O$, 0.12 g $Zn_5O_4{\cdot}7H_2O$, 0.15 g $CoC1_2{\cdot}6H_2O$ and 10 g Ethylenediamine tetra-acetic acid (EDTA)

[24]. This synthetic wastewater employed NaAc as carbon source as it is easy to be degraded and in favour of electricity-producing microbes enrichment. A phosphate buffer solution served to adjust the pH of the system. The influent of the anode chamber was the same as the cathode except for ammonium chloride. During the experiments, the anode chamber was operated in the intermittent operation mode, while operating the cathode chamber under the continuous mode. The solution in the anode chamber was replaced every 15 days to avoid the accumulation of sodium. The effluent in the cathode chamber was discharged from the system through an overflow channel. This period (from day 0 to 30) aims to enhance power generation and nutrient removal from the whole system. After a 30-day start-up procedure, the performance of the EAM-MFC was assessed at 28 ºC for 75 days under open circuit and at various external resistances (in 100 Ω, 50 Ω, 10Ω, 5 Ω, 0 Ω conditions, respectively).

2.3. Analytical methods

2.3.1. Electrochemical analyses

The voltage (U) across the resistance was recorded per 10 minutes employing a data acquisition system (Agilent 34970A, Agilent Co., USA). The electrode potential (ε) was measured by Ag/AgCl (assumed to be + 0.197 V vs SHE) (model 218, LeiCi) which were put in the anode and cathode chambers as two reference electrodes, respectively, and also detected with a multimeter. The current (I) and the power (P) can be described by Eqs. (1) and (2), respectively:

$$I = U/R \quad (1)$$

$$P = IU \quad (2)$$

where U is the measured voltage (V), and R the external resistance (Ω).

And the *coulombic efficiency (CE)* is given by Eq. (3)

$$CE = C_p/C_{th} \times 100\% \quad (3)$$

where C_p is the total coulombs calculated by integrating the current over time, and C_{th} is the theoretical amount of coulombs available based on the COD removed from the anodic chamber over the same period of time. The *coulombic efficiency (CE)* of nitrate reduction in the cathode can be expressed as the following equation [25]:

$$\varepsilon_{NO_x} = \frac{I}{n\Delta C_{NO_x} Q_{in} F} \times 100\% \quad (4)$$

Where I is the current (A), n is the number of electrons that can be accepted by 1 mol of oxidised nitrogen compound present in the cathode chamber assuming N_2 is the final product. Hence 5 for nitrate and 3 for nitrite (e-mol); ΔC_{NOx} is the difference between the nitrate (or nitrite) concentration in the cathodic influent and in the effluent (mol NL^{-1}); Q_{in} is the influent flow rate (L s^{-1}) and F is Faraday's constant (96485 C e-mol^{-1}). Linear sweep voltammetry was conducted to determine polarization curves. The current density and power density were obtained by Linear sweep voltammetry in a CHI604D electrochemical workstation (CH Instruments, Chenhua Instrument Co., Shanghai, China). The scan rate of the Linear sweep voltammetry was 1 mV s^{-1} and the maximum power density was obtained by analyzing the polarization curves [26].

2.3.2. Chemical analyses

Water samples were collected from influent and effluent from each chamber on a daily basis. All the samples were collected in triplicate and the figures were used the average value. The samples were analyzed for COD, NH_4^+-N, NO_2^--N, NO_3^--N and pH after being pretreated through 0.45 µm filter unit (Millex Corp.). All the test methods

were carried out using the standard methods with a HACH DR/6000 colorimeter.

3. Results and discussion

3.1. Start- up procedure

The EAM-MFC's generation of electricity during the start-up period is illustrated in Fig. 2(A). The reactors were firstly conducted under batch-fed mode (10 d) with external resistance of 1000 Ω to inoculate the microorganisms in both chambers. The electron supply or demand at the electrode surfaces determined the potentials of anode and cathode. The potential of the anode was maintained at a stable level of -290 ± 8.27 mV vs SHE after 10 days acclimated to the environment, which was ascribed to that sodium acetate was the major electron donor in the anode chamber. Thus the potential of the anode was fitted with that of acetate reduction ($E^0_{HCO3/CH3COO}$ = -290 mV vs standard hydrogen electrode, SHE). On the other hand, the potential of the cathode was initially around -200 ± 7.41 mV vs SHE, followed by a significant fluctuation, which then reached a higher potential on day 10, which in turn increased the voltage of the whole system. The maximum voltage output reached 469 mV (1000 Ω) after a 15-day start-up period. Then the external load was exchanged to 100 Ω, and the MFC voltage decrease was followed by a gradual increase. Finally, it stabilized at around 350 ± 12.88 mV.

Fig. 2 (A).

The removal rates of COD and NH_4^+-N were improved during the operation. At the end of the start-up stage the average removal rates of COD and NH_4^+-N were 61.53 ± 2.24% and 77.32 ± 2.63%, respectively. After 10 days the carbon and nitrogen removal

rate stabilized.

3.2. The system's electricity generation performance

3.2.1. The potential and voltage of the system

Fig. 2(B). illustrates the potential and voltage exchange under various external loads from 100 Ω to 0 Ω (considered as open circuit). In the start-up period the maximum voltage output reached 417 mV (1000 Ω). The EAM-MFC's electrochemical performance at different resistances was evaluated under continuous mode (cathode chamber). At first the voltage output decreased sharply and then increased rapidly, finally fluctuating slightly at a stable voltage of 350 mV at a resistance of 100 Ω. During the experiment, the potential of the anode was always maintained at about 290 mV, and this outcome indicated that the anode biofilm could generate power, and the reaction of sodium acetate was reduced; this was the main reaction around the anodic electrode [26]. This reaction was irrelevant to the external loads. As Zhu [27] reported, when the acetate concentration reached a stable level, the electro-microorganism activity attained the steady state, leading to a constant power generation. A similar finding was reported by Wang [28], which was demonstrated that solution could be continuously migrated with electrons from anode to cathode in the presence of adequate nutrients.

Fig. 2 (B).

Conversely, the potential of the cathode made an impact on the fluctuation in cell voltage. The maximum potential of the cathode was 0.18 V vs SHE, and this was still lower than the expected value of oxygen (0.805 V), nitrate (0.433 V) or nitrite (0.350 V) being reduced, thus indicated that a large energy loss occurred at the cathode. This energy loss is often considered as overpotential or explained by the difference between potentials under the standard condition and those under the actual condition [29]. The high overpotential was also affected by intermediate products (NO_2 and N_2O) generated during denitrification process and the potential which was utilized by microorganisms for their growth, activation and maintenance. The result was also reported in elsewhere [31, 31, 32]. In our research, the competition of different electron acceptors resulted in different reduced potential that might cause the fluctuation in cathodic potential. The poorer potential of the cathode in the coupled system is one of the factors causing the loss of power generation in compared with the other configured MFC.

3.2.2. Power density generated at different external loads

At the end of each run, the polarization curves and power density at different resistances were quantified to evaluate the electricity-producing ability of the coupled system. Fig. 3 illustrates variation of power density and polarization curves of the EAM-MFC coupled system at different external loads in the continuous operation mode. The best performance of power density (4.20 ± 0.12 W m^{-3} obtained at a current density of 4.10 ± 0.11 A m^{-2}) was given at an external load of 10 Ω. The power density decreased with deceasing the external loads while the current density performed in the opposite way. The maximum power density and open circuit voltage changed slightly when external loads were 100 Ω and 50 Ω. However, maximum power density at the

external resistance of 5 Ω was higher than 50% at the resistance of 100 Ω. The maximum power density of the EAM-MFC was higher than that of IEM-less system and the coupled system of MFC and aerobic activated sludge in previous studies (Wang [28] and Zhu [27]). The power densities of MFCs were correlated with internal resistances, and solution conditions tolerated by microorganisms, substrate degradability, and biofilm kinetics. Lower power densities were due to declined kinetics of biodegradation of complex substrates, decreased solution conductivities and reduced buffer capacity.

Fig. 3.

3.3. The removal of pollutants under different operating conditions

3.3.1. The removal rate of COD in each chamber of the system

The performance of the system was evaluated in terms of COD removal efficiency when treating synthetic wastewater. In this research, the different external resistances of the EAM-MFC system were employed to determine the removal efficiencies and coulombic efficiency of acetate. The changes in concentrations of COD along the reactor path are shown (Fig. 4A) during the continuous mode of different external loads. In the anodic chamber, the COD removal rate improved along with the decline in external loads. In this system, the current generated was all due to the acetate being reduced in the anodic chamber. As the external resistances decreased the current increased, suggesting that more effective electron transfers were needed and this led to higher removal rate of COD. The results indicated that a bio-electrochemical state wielded a positive influence on anode COD reduction. This finding was similar to the research by Tian [32]. However, in the cathode chamber, it seems it had no influence in

the removal rate of acetate-COD. The removal rates of the influent acetate-COD were similar in every operational stage. Except the closed circuit operated condition with the open circuit condition, a slight improvement in COD removal (about 25.85 ± 0.99%) was observed in the cathode chamber (Fig. 4B). In the closed circuit, the microorganisms on the anodic carbon felt was not only reduced organic matter metabolically, but also supplied electrons to the cathodic reaction. Thus the COD removal rate of anode improved. In contrast, microorganisms in the cathode chamber received extra electrons supplied from the anode, thus reducing the biodegradation of sodium acetate used for generating feed electrons, which decreased COD removal rate.

Fig. 4.

The efficiency of the anodic chamber under different aeration intensities (30 kPa, 20 kPa) and external loads (100 Ω, 50 Ω, 10 Ω, 5 Ω) is illustrated in Table 1. The EAM-MFC system was accomplished a maximal nominal current of 22 mA by applied a 5 Ω external resistance. When the current was changed from 3.60 mA to 22.00 mA, the coulombic efficiency of anodic acetate oxidation ranged from 8.91% to 40.67%, which was much higher than the value of the MFC-MBR system proposed by Tian [33] and Wang [34], and the IEM-less MFC (Zhu [27]). There were many factors influencing the coulombic efficiency of the anode, such as the diffused dissolved oxygen from the cathode chamber, fermentation and methanogenesis of some other bacteria in the anodic chamber [2, 3, 11]. As shown in Table 1, a comparison of the different aeration intensities was made to describe the advantage of electroconductivity MABR as the cathode chamber. At higher aeration intensity, more oxygen could serve as electron acceptors and the voltage ascended accordingly.

Table 1.

However, there was little influence in anode coulombic efficiency (just 0.34% decrease). There were two important advantages to achieving better coulombic efficiency: Firstly, the favorable control of aerate in cathode chamber (electroconductivity MABR) and the layering of the biofilm can make the most use of oxygen and thus avoid the dissolved oxygen diffusing to the anodic chamber. Further, most of the microorganisms in the anode chamber were adsorbed on the surface of graphite felt at the anode so as they resulted in a higher utilization rate of organic reduction. When increasing the external resistances, the electron transfer from the anode biofilm could become limited, thus compromising the MFCs electron transfer and accordingly decreasing the anode's coulombic efficiency. In conclusion, the COD removal efficiencies by the anodic chamber in the EAM-MFC were 67.01%-98.66%, which mainly contained the COD recovery as electricity (9.27%-40.67%) and metabolization of COD by the electrostactic bacteria and other bacteria [34].

3.3.2. The removal rate of nitrogen

In this research, the most important thing was improving SND in the single chamber. Measurements of concentrations of ammonium, nitrate and nitrite in the influent and effluent were performed to monitor total nitrogen (TN) removal efficiencies in the MFCs (Fig. 5). The nitrogen removal rate increased gradually in the cathode, along with a decrease in the external loads which promoted the electrochemical denitrification. At the beginning of the experiment (with external resistance at 1000 Ω) the nitrate concentration slightly increased and then at the resistance of 100 Ω the

concentration rapidly decreased as the resistance diminished. This indicated that the increase in the current generated more electron transfer through the circuit in unit time, which made the degradation rate of COD in the anode chamber increased and caused the reaction of denitrification in the cathode chamber. The result was consistent with the findings of Zhang [36]. During the operation at an external resistance of 5 Ω, the nitrogen content in the effluent was as low as 12.93 mg NH_4^+-N L^{-1}, 0.12 mg NO_3^--N L^{-1} and 2.18 mg NO_2^--N L^{-1}, thus resulting in the highest measured NH_4^+-N removal efficiency of 80.90% at a removal rate of 0.16 kg N m^{-3} NCC d^{-1}.

Fig. 5.

In addition, the nitrate was electrochemically eliminated in the cathode using electrons obtained via acetate oxidation in the anodic chamber. Firstly, the effluent of nitrite was barely detected, but after decreasing the external loads the nitrite gradually accumulated and finally reached around 2.32 mg L^{-1}. This means that when more nitrate was reduced then more nitrite accumulated if it exceeded the maximum reduction capacity. The total nitrogen removal in the cathode chamber was investigated using ammonia nitrogen, nitrate and nitrite. The TN removal efficiency in the cathode chamber was 80.80% with accumulation of few nitrate and only a little nitrite due to the electrochemically biological denitrification. Maximum removal rates were attained up to 0.390 kg COD m^{-3} d^{-1} and 0.128 kg TN m^{-3} d^{-1}, resulting in a maximal COD and TN removal efficiency of 94.74% and 80.82%, respectively. When comparing the open circuit to external resistance at 5 Ω the removal rate improved by nearly 19.80%. This improvement was less than that accomplished by Zhu [27] who reported the removal efficiency of TN was 2.6 times greater than open-circuit state, and also lower than a

single chamber microbial fuel cell with a rotating biocathode [36]. This improved the removal rate of TN by 22.71% in the closed circuit scenario.

There were two reasons for the poorer improvement in our system. Firstly, some of the electrons from anode reacted with the oxygen in the cathode chamber and produced water, thus reducing the amounts of electrons for denitrification. Apart from that, the insufficient supply of electrons limited the higher removal rate of TN. Furthermore, by calculating the organic matter and ammonia consumed by EAM-MFC, the COD/N ratio was just 1.875 ± 0.05 g COD g^{-1} NH_4^+-N. The ratio was lower than half of the C/N ratio for traditional MABR (5 g COD g^{-1} NH_4^+-N) [37] and was lower than the research of Zhao et al. which was developed a novel sludge system to treat a low C/N (4.03) wastewater [38]. As considered there was 40.67 ± 1.25% COD removed from the anodic chamber (data from the anode's former coulombic efficiency, electrons were supplied for electrochemical denitrification in the cathode. The COD/N ratio increased only a little to 2.89 ± 0.08 g COD g^{-1} NH_4^+-N, and this result is still lower than the research on cathodic nitrate reduction by Virdis [6] (4.5 g COD g^{-1} NH_4^+-N). In recently study, Guo [39] used a complicated sequencing batch reactor reached a low COD/TN ratio of 2 - 3.

As shown in Fig. 6, the mechanisms of TN removal in the cathode chamber are possibly responsible for the explanation posited by Clauwaert et al. [5] and Tian et al. [32]: (1) utilization of oxygen by nitrifying organisms in the inner layer of the biofilm for nitrification; and (2) migration of electrons by the electroactive bacteria from inside to the outside of the electrode for anaerobic denitrifying bacteria to accomplish denitrification process. The result of Xiao et al. [40] showed that electrons can be transferred between electrode and biofilm, and nitrate may be removed by heterotrophic biofilm using electrode as electron donor. In addition, some heterotrophic bacteria may

used degrade dead cells as carbon sources for nitrate reduction [41]. In summary, the coupled system made the most use of electrons from the anode and this delivered superior COD and nitrogen removal performance at low COD/N influent in different running scenarios.

Fig. 6.

Table 2 illustrates the coulombic efficiency of cathodic NO_3^--N and NO_2^--N. The external resistances strongly limited the electron transfer thus influenced the electrochemical denitrification performance and coulombic efficiency of the cathode. As the external resistances decreased the increase of current accordingly, more effective electron transfers were needed. This was in some way resulted in better denitrification and improved coulombic efficiency of the cathode. A similar result was found in a previous study [2]. Many factors (e.g. substrate consumption for methanogenesis, the electrons transporting from the substrate to other electron acceptors) will influence the cathode coulombic efficiency of EAM-MFC. The coulombic efficiency reduction of the EAM-MFC was mainly due to electrons utilized by denitrifying bacteria for their growth.

Table 2.

4. Conclusions

In this study, an innovative coupled EAM-MFC system was operated, the maximum denitrification rate of 80.81% (0.128 kg TN m^{-3} d^{-1}) and a maximum COD removal rate of 94.73% (0.34 kg COD m^{-3} d^{-1}) were achieved at C/N ratio of 2.89 g COD g^{-1} NH_4^+-N. The nitrogen removal rate was improved 19.80 ± % in the closed

circuit scenario. The current density increased with decreasing the external loads, which reduced the accumulation of nitrate and nitrite. These results demonstrated that this system has the potential to reduce organic materials and improves nitrogen removal while recovering energy in the form of electricity and thus reducing the system's operational costs.

Acknowledgement

This work was financially supported by the Chinese National Natural Science Foundation [No. 51678410], Postdoctoral Science Foundation of China [No. 2015M571267] and major R&D Projects of Tianjin of China [No. 14ZCDGSF00128]. The authors are also grateful for the research collaboration between Tianjin Polytechnic University and University of Technology Sydney, especially on the Opening Research Fund of State Key Laboratory of Hollow Fiber Membrane Materials and Processes, 2016.

References

[1] P. Aelterman, K. Rabaey, H.T. Pham, N. Boon, W. Verstraete, Continuous electricity generation at high voltages and currents using stacked microbial fuel cells, Environmental Science &Technology. 40 (2006) 3388 - 3394.

[2] H. Liu, B.E. Logan, Electricity generation using an air-cathode single chamber microbial fuel cell in the presence and absence of a proton exchange membrane, Environmental Science &Technology. 38 (2004) 4040 - 4046.

[3] B.E. Logan, B. Hamelers, R. Rozendal, U. Schröder, J. Keller, S. K. Freguia, Rabaey, Microbial fuel cells: methodology and technology, Environmental Science

&Technology. 40 (2006) 5181 - 5192.

[4] K. Rabaey, W. Verstraete, Microbial fuel cells: novel biotechnology for energy generation, TRENDS in Biotechnology. 23 (2005) 291 - 298.

[5] P. Clauwaert, K. Rabaey, P. Aelterman, L. De Schamphelaire, T.H. Pham, P. Boeckx, W. Verstraete, Biological denitrification in microbial fuel cells, Environmental Science &Technology. 41 (2007) 3354 - 3360.

[6] B. Virdis, K. Rabaey, Z. Yuan, J. Keller, Microbial fuel cells for simultaneous carbon and nitrogen removal, Water Research. 42 (2008) 3013 - 3024.

[7] C.P. Yu, Z. Liang, A. Das, Z. Hu, Nitrogen removal from wastewater using membrane aerated microbial fuel cell techniques, Water Research. 45 (2011) 1157 - 1164.

[8] A. Vilajeliu-Pons, S. Puig, N. Pous, Microbiome characterization of MFCs used for the treatment of swine manure, Journal of Hazardous Materials. 288 (2015) 60 - 68.

[9] Q. Tao, J. Luo, J. Zhou, Effect of dissolved oxygen on nitrogen and phosphorus removal and electricity production in microbial fuel cell, Bioresource Technology. 164 (2014) 402 - 407.

[10] D. Jiang, M. Curtis, E. Troop, A pilot-scale study on utilizing multi-anode/cathode microbial fuel cells (MAC MFCs) to enhance the power production in wastewater treatment, Fuel & Energy Abstracts. 36 (2011) 876 - 884.

[11] Y.P. Wang, X.W. Liu, W.W. Li, F. Li, Y.K. Wang, G.P. Sheng, H.Q. Yu, A microbial fuel cell-membrane bioreactor integrated system for cost-effective wastewater treatment, Applied Energy. 98 (2012) 230 - 235.

[12] E.V. Münch, P. Lant, J. Keller, Simultaneous nitrification and denitrification in

bench-scale sequencing batch reactors, Water Research. 30 (1996) 277 - 284.

[13] K. Pochana, J. Keller, Study of factors affecting simultaneous nitrification and denitrification (SND), Water Science and Technology. 39 (1999) 61 - 68.

[14] G. Zhu, G. Chen, R. Yu, H. Li, C. Wang, Enhanced simultaneous nitrification/denitrification in the biocathode of a microbial fuel cell fed with cyanobacteria solution, Process Biochemistry. 51 (2016) 80 - 88.

[15] A. Sotres, M. Cerrillo, M. Viñas, Nitrogen removal in a two-chambered microbial fuel cell: Establishment of a nitrifying-denitrifying microbial community on an intermittent aerated cathode, Chemical Engineering Journal. 285 (2016) 905 - 916.

[16] B. Virdis, K. Rabaey, R.A. Rozendal, Z. Yuan, J. Keller, Simultaneous nitrification, denitrification and carbon removal in microbial fuel cells, Water Research. 44 (2010) 2970 - 2980.

[17] K. Soejima, S. Matsumoto, S. Ohgushi, K. Naraki, A. Terada, S. Tsuneda, A. Hirata, Modeling and experimental study on the anaerobic/aerobic/anoxic process for simultaneous nitrogen and phosphorus removal: The effect of acetate addition, Process Biochemistry. 43 (2008) 605 - 614.

[18] G. Zhang, H. Zhang, Y. Ma, G. Yuan, F. Yang, R. Zhang, Membrane filtration biocathode microbial fuel cell for nitrogen removal and electricity generation, Enzyme and Microbial Technology. 60 (2014) 56 - 63.

[19] C. Sukkasem, S. Xu, S. Park, P. Boonsawang, H. Liu, Effect of nitrate on the performance of single chamber air cathode microbial fuel cells, Water Research. 42 (2008) 4743 - 4750.

[20] J. Wang, F. Bi, H.H. Ngo, W. Guo, H. Jia, H. Zhang, X. Zhang, Evaluation of energy-distribution of a hybrid microbial fuel cell–membrane bioreactor (MFC–MBR)

for cost-effective wastewater treatment, Bioresource Technology. 200 (2016) 420 - 425.

[21] G. Zhou, Y. Zhou, G. Zhou, L. Lu, X. Wan, H. Shi, Assessment of a novel overflow-type electrochemical membrane bioreactor (EMBR) for wastewater treatment, energy recovery and membrane fouling mitigation, Bioresource Technology. 196 (2015) 648 - 655.

[22] W. Li, S. Zhang, G. Chen, Y. Hua, Simultaneous electricity generation and pollutant removal in microbial fuel cell with denitrifying biocathode over nitrite, Applied Energy. 126 (2014) 136 - 141.

[23] J. Li, G. Rosenberger, Z. He, Integrated experimental investigation and mathematical modeling of a membrane bioelectrochemical reactor with an external membrane module, Chemical Engineering Journal. 287 (2015) 321 - 328.

[24] L.T. Angenent, S. Sung, Development of anaerobic migrating blanket reactor (AMBR), a novel anaerobic treatment system, Water Research. 35(2001) 1739 - 1747.

[25] G. Zhu, T. Onodera, M. Tandukar, S.G. Pavlostathis, Simultaneous carbon removal, denitrification and power generation in a membrane-less microbial fuel cell, Bioresource Technology. 146 (2013) 1 - 6.

[26] N. Pous, S. Puig, M.D. Balaguer, J. Colprim, Cathode potential and anode electron donor evaluation for a suitable treatment of nitrate-contaminated groundwater in bioelectrochemical systems, Chemical Engineering Journal. 263 (2015) 151 - 159.

[27] P. Clauwaert, Ha.D. Van der, N. Boon, K. Verbeken, M. Verhaege, K. Rabaey, W. Verstraete, Open air biocathode enables effective electricity generation with microbial fuel cells, Environmental Science & Technology. 41 (2007) 7564 - 7569.

[28] H. Wang, S.C. Jiang, Y. Wang, B. Xiao, Substrate removal and electricity generation in a membrane-less microbial fuel cell for biological treatment of wastewater,

Bioresource Technology. 138 (2013) 109 - 116.

[29] S. Puig, M. Coma, J. Desloover, N. Boon, J. Colprim, M.D. Balaguer, Autotrophic denitrification in microbial fuel cells treating low ionic strength waters, Environmental Science &Technology. 46 (2012) 2309 - 2315.

[30] B.E. Logan, K. Rabaey, Conversion of wastes into bioelectricity and chemicals by using microbial electrochemical technologies, Science. 337 (2012) 686 - 690.

[31] B. Min, I. Angelidaki, Innovative microbial fuel cell for electricity production from anaerobic reactors, Journal of Power Sources. 180 (2008) 641 - 647.

[32] Y. Tian, C. Ji, K. Wang, P. Le-Clech, Assessment of an anaerobic membrane bio-electrochemical reactor (AnMBER) for wastewater treatment and energy recovery, Journal of Membrane Science. 450 (2014) 242 - 248.

[33] Y. Tian, H. Li, L. Li, X. Su, Y. Lu, W. Zuo, J. Zhang, In-situ integration of microbial fuel cell with hollow-fiber membrane bioreactor for wastewater treatment and membrane fouling mitigation, Biosensors and Bioelectronics. 64 (2015) 189 - 195.

[34] Y.K. Wang, G.P. Sheng, W.W. Li, Y.X. Huang, Y.Y. Yu, R.J. Zeng, H.Q. Yu, Development of a novel bioelectrochemical membrane reactor for wastewater treatment, Environmental Science &Technology. 45 (2011) 9256 - 9261.

[35] X. Su, Y. Tian, Z. Sun, Y. Lu, Z. Li, Performance of a combined system of microbial fuel cell and membrane bioreactor: wastewater treatment, sludge reduction, energy recovery and membrane fouling, Biosensors and Bioelectronics. 49 (2013) 92 - 98.

[36] G. Zhang, H. Zhang, C. Zhang, G. Zhang, F. Yang, G. Yuan, F. Gao, Simultaneous nitrogen and carbon removal in a single chamber microbial fuel cell with a rotating biocathode, Process Biochemistry. 48 (2013) 893 - 900.

[37] T. Zhu, Y. Zhang, X. Quan, Effects of an electric field and iron electrode on anaerobic denitrification at low C/N ratios, Chemical Engineering Journal. 266 (2015) 241 - 248.

[38] W. Zhao, Y. Zhang, D. Lv, Advanced nitrogen and phosphorus removal in the pre-denitrification anaerobic/anoxic/aerobic nitrification sequence batch reactor (pre-A 2 NSBR) treating low carbon/nitrogen (C/N) wastewater, Chemical Engineering Journal. 302 (2016) 296 - 304.

[39] Y. Guo, Y. Peng, B. Wang, Achieving simultaneous nitrogen removal of low C/N wastewater and external sludge reutilization in a sequencing batch reactor, Chemical Engineering Journal. 306 (2016) 925 - 932.

[40] Y. Xiao, S. Wu, Z.H. Yang, In situ, probing the effect of potentials on the microenvironment of heterotrophic denitrification biofilm with microelectrodes, Chemosphere. 93(2013) 1295 - 300.

[41] Y. Xiao, Y. Zheng, S. Wu, Bacterial Community Structure of Autotrophic Denitrification Biocathode by 454 Pyrosequencing of the 16S rRNA Gene, Microbial Ecology. 69 (2015) 492-499.

Table titles

Table 1. Summary of the parameters used to describe the electrical performance of the EMA-MFC coupled system at different external loads.

Table 2. Summary of the parameters used to describe the electrical performances of the cathodic chamber in the EMA-MFC coupled system at different external loads.

Table 1.
Summary of the parameters used to describe the electrical performance of the EAM-MFC coupled system at different external loads.

Resistance (Ω)	100	100	50	10	5
Aeration Intensity (kPa)	30 ± 1.14	20 ± 0.76	20 ± 0.76	20 ± 0.76	20 ± 0.76
Voltage (mV)	387 ± 15.29	360 ± 12.57	300 ± 10.93	205 ± 7.11	110 ± 3.29
DO of Anode (mg l^{-1})	0.38 ± 0.01	0.24 ± 0.01	0.21 ± 0.01	0.22 ± 0.01	0.21 ±0.01
Current (mA)	3.87 ± 0.15	3.60 ± 0.13	6.00 ± 0.11	20.50 ± 0.07	22.00 ± 0.03
Current density (A m^{-2})	0.76 ± 0.03	0.72 ± 0.03	1.20 ± 0.02	4.10 ± 0.01	4.40 ± 0.01
Power density (W m^{-3})	1.43 ± 0.15	1.30 ± 0.13	1.80 ± 0.11	4.20 ± 0.07	2.42 ± 0.03
COD removal rate of anode (mg L^{-1})	147 ± 3.28	134 ± 4.23	151 ± 3.75	191 ± 4.49	196 ± 3.90
CE of anode (%)	9.27 ± 0.33	9.61 ± 0.38	14.42 ± 0.27	38.90 ± 0.49	40.67 ±1.25

Table 2.
Summary of the parameters used to describe the electrical performances of the cathodic

chamber in the EAM-MFC coupled system at different external loads.

Resistance (Ω)	100	50	10	5	Open circuit
Aeration Intention (kPa)	20 ± 0.76	20 ± 0.76	20 ± 0.76	20 ± 0.76	20 ± 0.76
Voltage (mV)	360 ± 12.57	300 ± 10.93	205 ± 7.11	110 ± 3.29	--
Current (mA)	3.60 ± 0.13	6.00 ± 0.11	20.50 ± 0.07	22.00 ± 0.03	--
Power density ($W\ m^{-3}$)	1.30 ± 0.13	1.80 ± 0.11	4.20 ± 0.07	2.42 ± 0.03	--
NO_3^--N, NO_2^--N removal rate ($mg\ L^{-1}$)	56.02 ± 1.47	58.43 ± 1.69	62.47 ± 2.33	64.81 ± 2.06	49.28 ± 1.58
CE of cathode (%)	8.11 ± 0.26	12.96 ± 0.0.44	41.45 ± 0.93	42.48 ± 0.89	--

Figure captions

Fig. 1. Schematic diagram of the EMA-MFC system.

Fig. 2. The potentials and the voltages of the coupled system during the start-up period (A) and at different external loads after start-up period (B).

Fig. 3. Variation of (A) power densities and (B) polarization curves of the EMA-MFC coupled system at different external loads.

Fig. 4. The removal rates of COD in (A) anodic and (B) cathodic chambers.

Fig. 5. The removal rate of nitrogen in the cathodic chamber.

Fig. 6. Schematic diagram of nitrogen removal in the cathodic chamber.

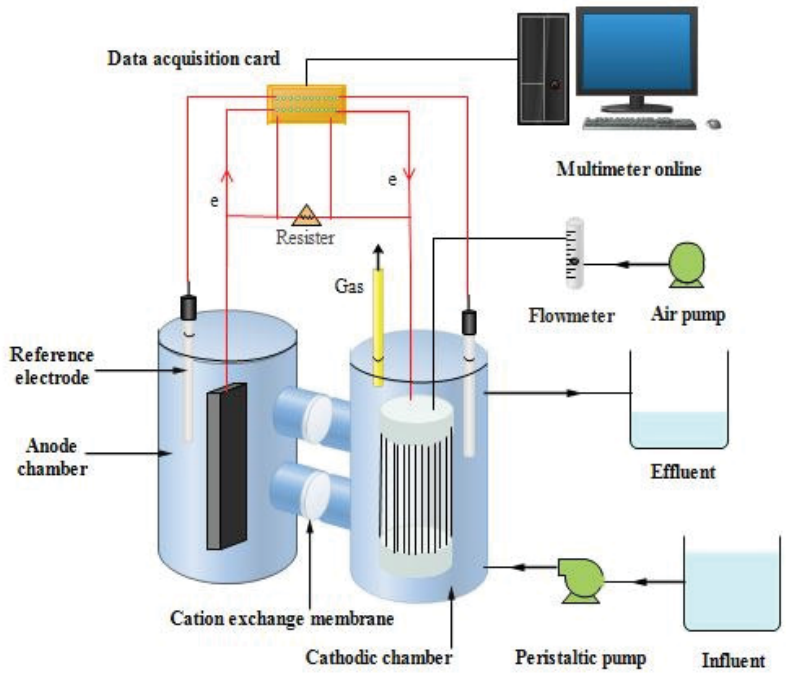

Fig. 1.

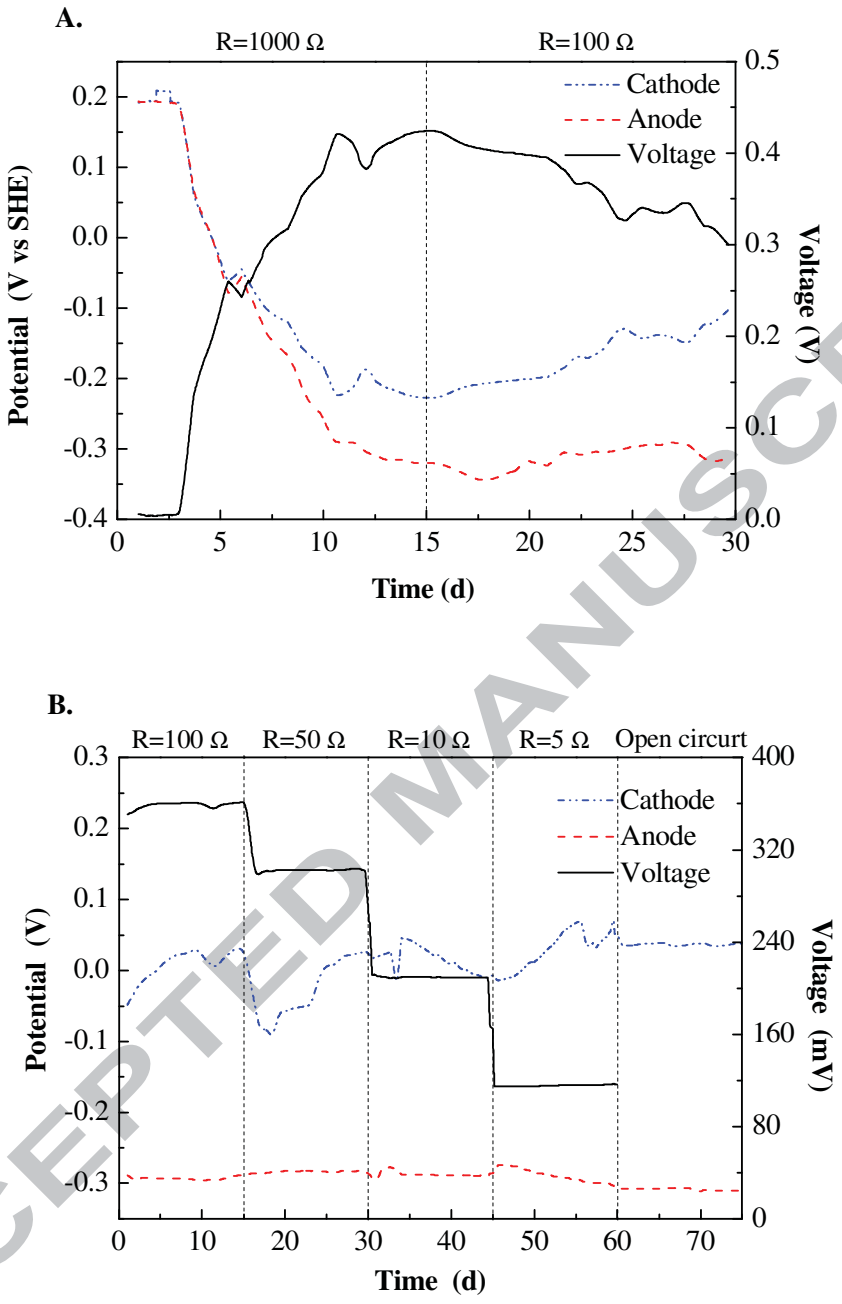

Fig. 2.

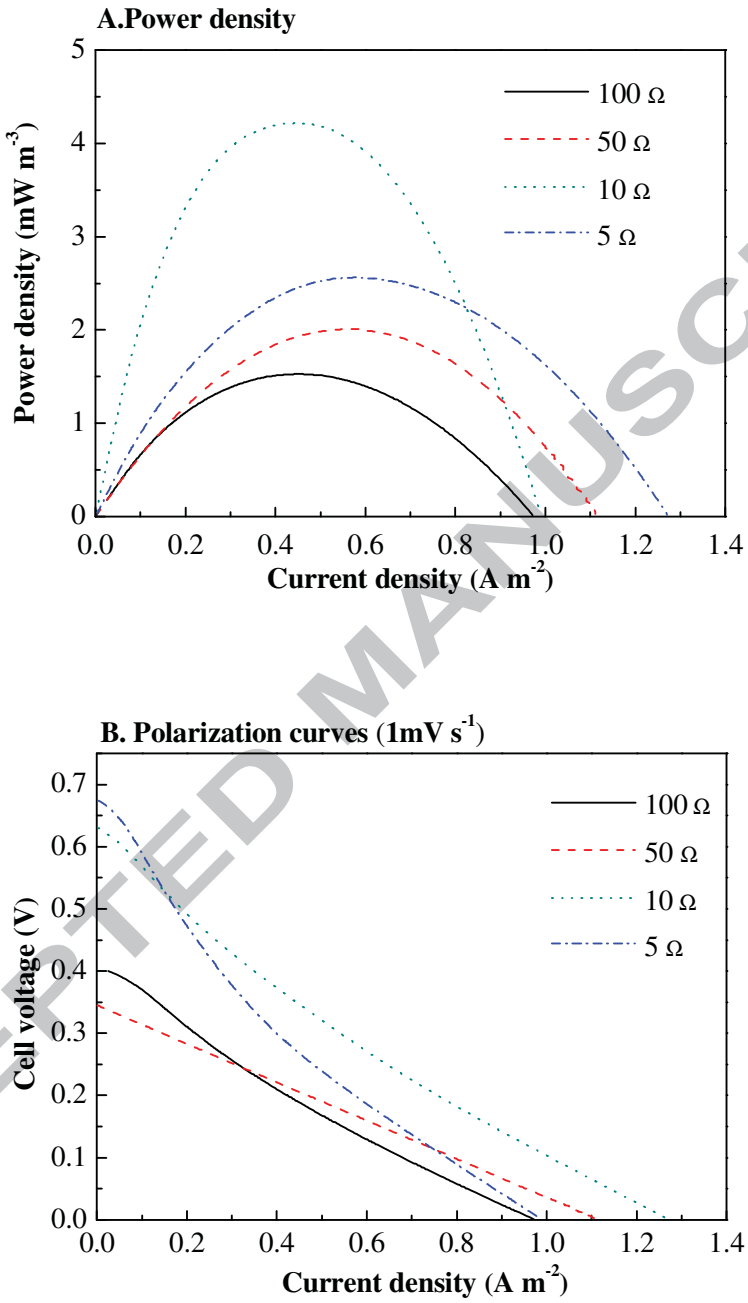

Fig. 3.

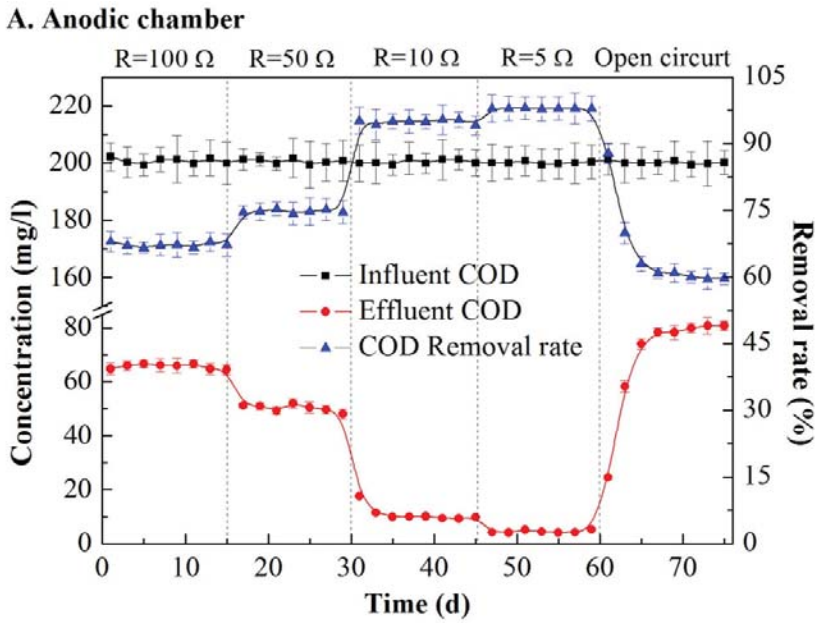

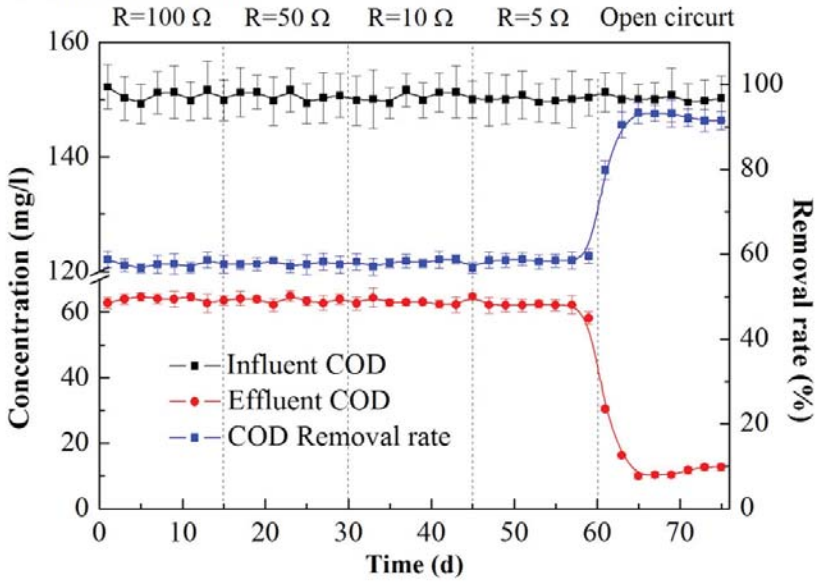

Fig. 4.

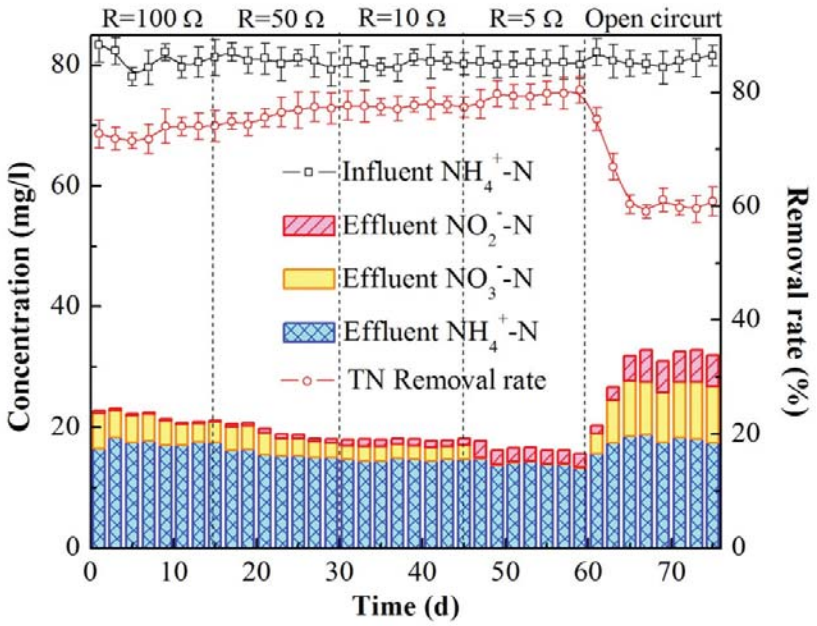

Fig. 5.

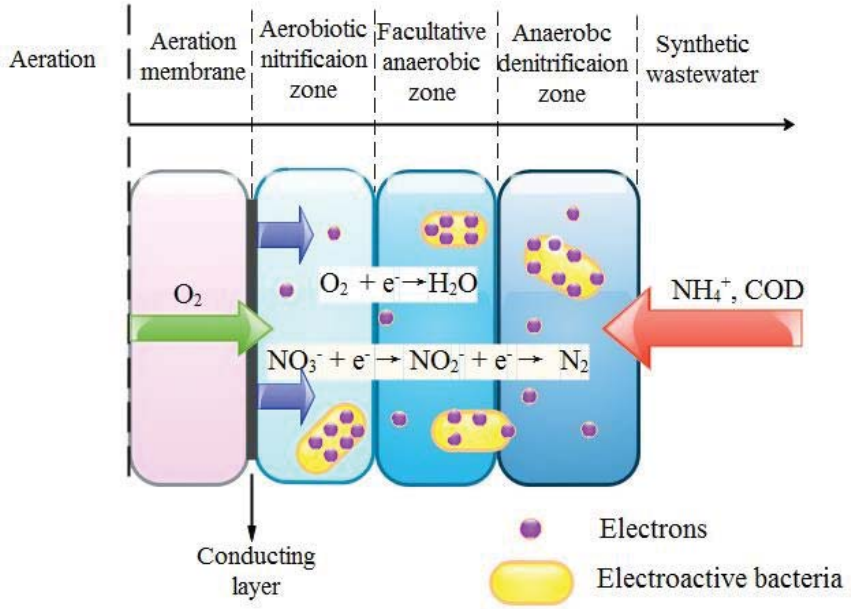

Fig. 6.

Graphic abstract

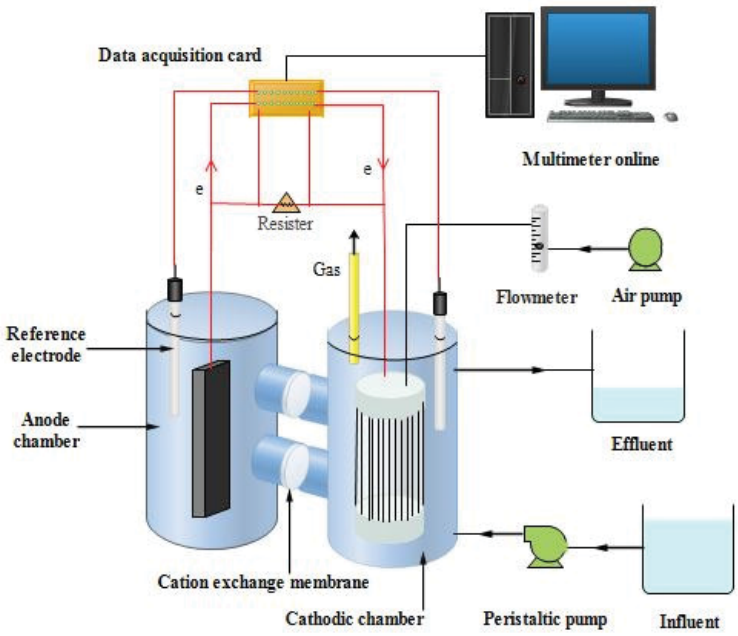

Highlights

- An Electroconductivity aerated membrane (EAM) - microbial (MFC) system was developed.
- The EAM-MFC system improved simultaneous nitrification denitrification rate.
- The EAM - MFC system obtained the maximum denitrification rate at low C/N ratio of 2.8.
- Simultaneous bio-electrochemical denitrification promoted nitrogen removal rate.
- The EAM-MFC enhanced the coulombic efficiency of the cathode.